MODEL STUDIES FOR THE SUPERCONDUCTING CYCLOTRON PROJECT IN MILAN

E. Acerbi, G. Bellomo, M. Castiglioni, C. de Martinis, E. Fabrici, C. Pagani, and F. Resmini
University of Milan and Istituto Nazionale di Fisica Nucleare, Milan, Italy

Introduction

Design study for a superconducting cyclotron started in Milan in 1975, the machine being intended as a booster for a 16 MV Tandem to be installed at the Legnaro Laboratories (Padua) of the Italian National Institute for Nuclear Physics (I.N.F.N.). A detailed analysis of all major physical and engineering aspects of the project was completed in June 1976.[1] In the meantime it was also decided that, pending approval and funding of the project, a model construction program would be helpful for i) getting the group acquainted with the problems connected with such a sophisticated machine, especially cryogenics and superconducting coil technology, ii) checking the theoretical calculations used for assessing magnetic fields and R.F. properties, and iii) ultimately reducing the time needed to build the machine in the near future.

Consequently, a program centered upon the construction of a 1:6 scale superconducting model magnet and a 1:1 scale R.F. cavity model was launched in 1976 and successfully completed toward the end of 1977. The purpose of this paper is to give a review of this program, its results, and the present status of the project.

Main Accelerator Characteristics

In order to put the model program in a proper perspective, we summarize the main goals of the project and the overall machine characteristics as they stand now. When combined with the 16 MV Tandem, the cyclotron will have T/A vs. A operating curves as shown in Fig. 1 for both the maximum and minimum energies. The former are between 70 MeV/n and 15 MeV/n for light and very heavy ions, respectively, corresponding to an effective K≈600 and a focusing $K_F \approx 140$. Some relevant design parameters are listed in Table I.

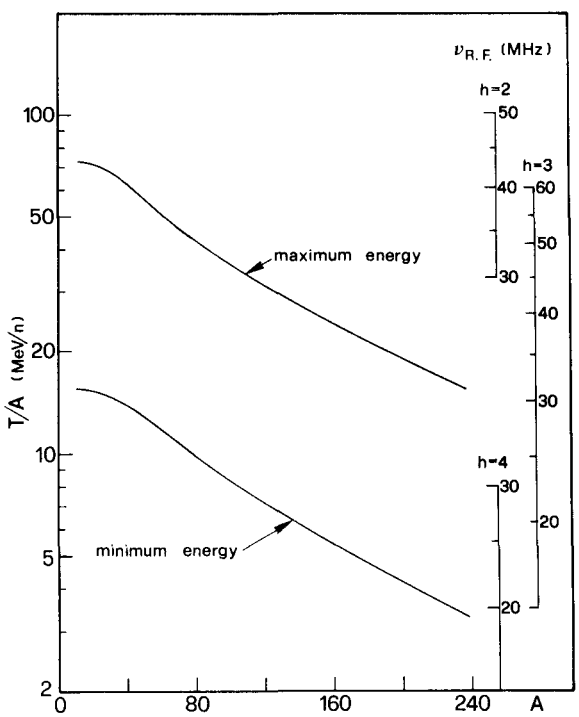

Fig. 1. Maximum and minimum energies per nucleon for the cyclotron when coupled to the 16 MV Tandem.

Table I. Main machine parameters

Pole diameter = 180 cm
Number of sectors = 3
Spiral constant = 1.6 and 1.8 rad/m^{-1}
Minimum hill gap = 7.2 cm
Valley gap = 60 cm
Main coils At = 6.4×10^6 at 3200 A/cm^2
Minimum and maximum average field = 23 and 43 kG
Yoke = threefold symmetry or closed (undecided)
Dees: 3, in valleys
Frequency range = 20 to 55 MHz
Operating harmonics: 2, 3, 4
Peak dee voltage = 100 kV
R.F. power = 3 x 50 = 150 kW

A layout of the proposed machine is shown in Fig. 2 for the threefold open yoke geometry. Actually, a closed yoke seems now the most likely choice. Injection trajectories originate from a common point about 3m downstream, where a steering magnet, not shown in the figure, provides the ±1.5° deviation needed to match the required injection paths for all particles and energies. Stripping is in a hill, with both azimuth and radius of the stripping foil being adjustable. The range of stripping radii is between 15 cm and 25 cm. Excitation of the $\nu_R=1$ resonance, as shown in Fig. 3 for a maximum energy light ion, provides enough turn separation for extraction. The latter, as schematically shown in Fig. 2, uses two electrostatic channels about 50° long positioned in two successive hills and operated typically at 140 kV/cm for 70 MeV/n light ions, and 100 kV/cm for 15 MeV/n uranium ions. A radially focusing magnetic channel , about 40° long and with gradients of 1.5 kG/cm, completes the extraction scheme.

A vertical cross section of the accelerator is shown in Fig. 4. The main coils, providing a total of 6.4×10^6 At, are split into two equal parts in order to isochronize the magnetic field with minimum trim coil power. Overall focusing properties of the magnetic field seem quite good, as shown in Fig. 5 for the cases of fully stripped light ions and uranium ions at their respective maximum energies.

The 1:6 Scale Superconducting Magnet

Various technical aspects of the model magnet design have been reported elsewhere.[2] In this section we shall therefore summarize only the main features of the project. As is well known, the main problem in building scaled down model magnets is the corresponding scaling up of the current density in the coils. For superconducting coils this is particularly difficult, since current densities close to critical values are soon reached. Choice of the scale factor is therefore a key issue, since a delicate compromise must be struck between costs and a reasonable chance of success. A 1:6 scale was selected, yielding a current density of ≈18.500 A/cm^2 at the maximum excitation. Every effort was then made to preserve an accurately scaled geometry of the proposed machine.

The corresponding parameters of the iron structure thus selected are listed in Table II.

0018-9499/79/0400-2048$00.75

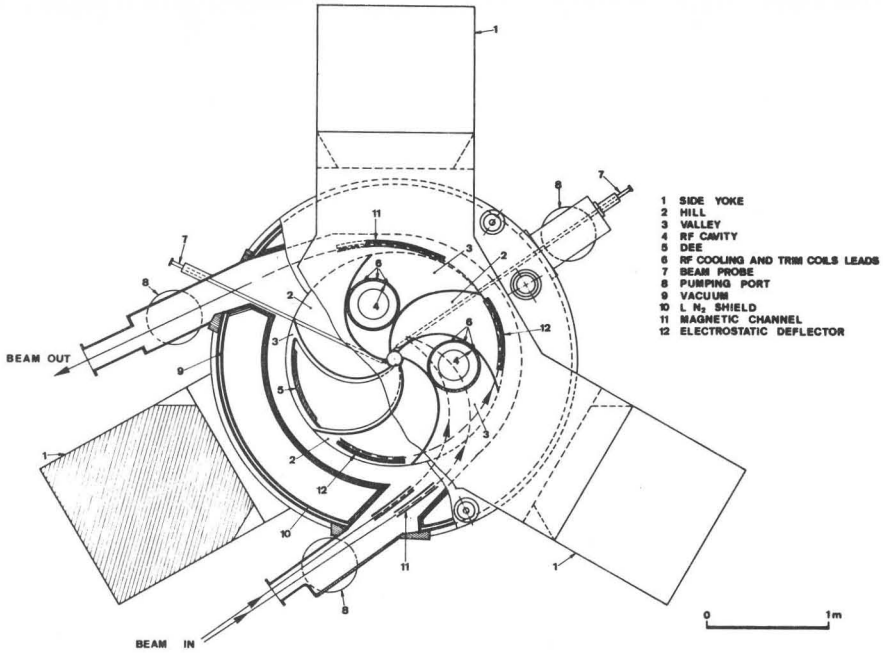

Fig. 2. Cyclotron layout in the threefold open yoke version.

Closed yoke geometry was ruled out, mainly because of the need of access to the cryostat body and long delivery time for the iron castings. As for the coil design, it was realized that splitting each coil into two independently excited sections, as needed in the real machine, would increase the cost considerably, while not adding substantial information to magnetic field studies. The coils were then designed according to the specifications set forth in Table III, and commissioned to Brown-Boveri Co., Oerlikon, Switzerland.

A cross section of the full magnet, including coils and cryostat, is shown in Fig. 6. As seen in detail in Fig. 7, both the upper and lower coil are split into two concentric parts (A, B_s series connected) for the purpose of better cooling. Copper coils C, shortcircuited inside the cryostat, have the purpose of disposing of part of the energy released in a quench. Quench detection coils (D) are also wound concentrically with the main coils. All these components are epoxy impregnated together with the fiberglass ring E. The coils are fixed to a central stainless steel ring, 84 mm thick, which disposes of compression forces by means of 48 titanium rods, 2 mm in diameter and 100 mm long. A picture of one of the coils, ready for mounting, is shown in Fig. 8.

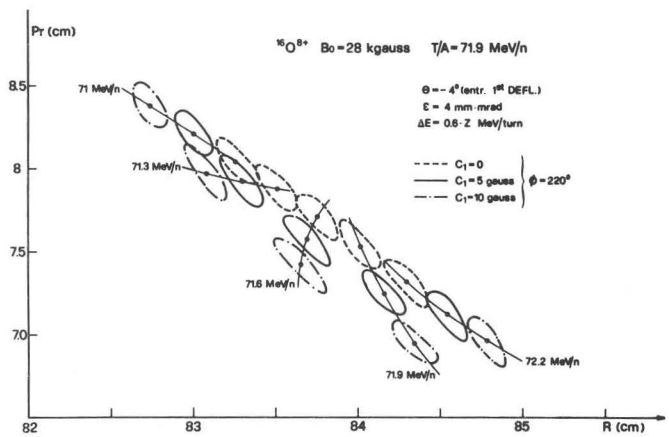

Fig. 3. Turn to turn separation pattern with excitation of ν_R=1 resonance.

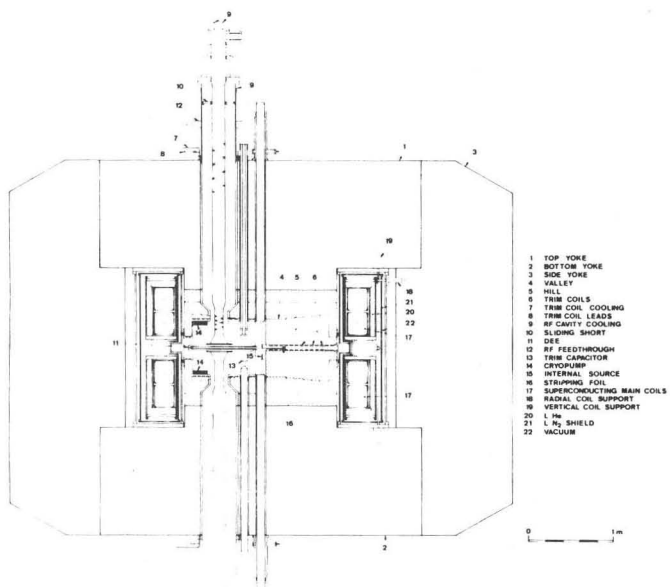

Fig. 4. Axial cross section of the cyclotron.

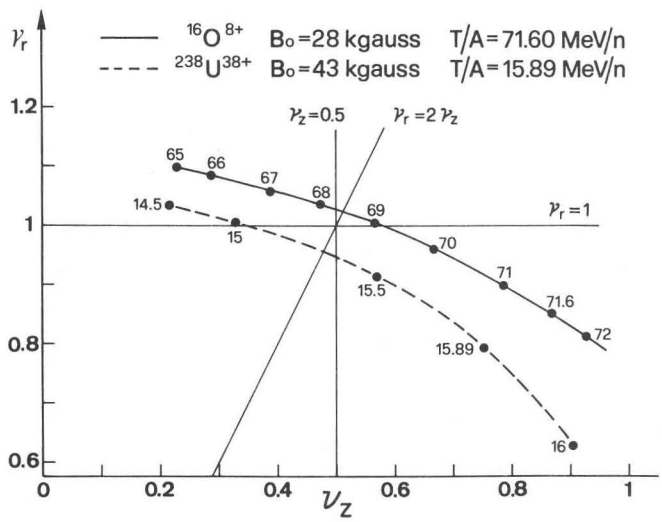

Fig. 5. Operating (ν_r,ν_z) diagram for light and heavy ion examples.

The coils are excited with an in-house built power supply, featuring 0.005% current stability and programmable current vs. time ramps of 30, 60, 80, 120, and 180 minutes. These figures refer to the time needed to reach the maximum coil excitation of 145 A. Details of the power supply, protection against quenches, and quench detection system (QDS) are found in Ref. 3. For the present purposes, it is useful to recall that the dump resistor, to which the coils are permanently connected, is of 26 ohm, so that voltages up to ≃4000 volts (145 A x 26 ohm) can be reached in case of quenches at high excitation. We were however prevented from using

0018-9499/79/0400-2049$00.75 ©1979 IEEE

lower resistance values by the fact that the large coil inductance (≈24 H) would entail too long discharge times and therefore hazards of coil overheating. Total intervention time of the quench detection system is about 60-80 msec, including the opening time of fast switches.

Table II. Model magnet iron structure

Upper, lower yoke = four fold, 19 cm thick, C 10 cast iron
Side yoke = 4 pieces, 19 x 19 x 87.3 cm^3, C 10 cast iron
Poles = ϕ30 cm, C 10 cast iron
Pole tips = 3 sectors, spiral (k=9.6 and 10.8 m^{-1}) Armco iron
Minimum hill gap = 12 mm
Maximum valley gap = 100 mm
Center hole = ϕ25 mm, (int. ion source hole)
Valley holes = ϕ41.6 mm, ϕ17 mm, (simulating dee stems, capacitors feedthroughs)
Iron weight = 2.1 tons
Overall dimensions = 104 x 104 x 87.8 cm

Table III. Superconducting coil parameters

Maximum excitation = 1 x 10^6 At
Conductor = NbTi, ϕ=.66 mm
Copper to superconductor ratio = 2.48:1
Critical current at 4.5 T, 4.2°K = 170 A
Operating max. current = 145.6 A
Number of turns = 2 x 3433
Max. current density = 18.500 A/cm^2
Stored energy = 250 kJoule
Coil inner diameter = 264 mm
Coil outer diameter = 466 mm
Coil height = 83 mm
Weight = 29 Kg /coil
Max. tensile stress = 11 Kg/cm^2

The cryostat's main features have been described elsewhere.[3] It consists basically of the liquid helium tank, a liquid nitrogen radiation shield, and the outer vacuum chamber. A picture of the completely assembled cryostat is shown in Fig. 9. The liquid helium tank, made of 216 L stainless steel and weighing 108 kg, is suspended from the outer vacuum chamber by 8 titanium alloy rods (6% Al, 4% Va), with a diameter of 5 mm and 30 cm long. The suspending structures can clearly be seen at 45° to the median plane, both in Fig. 6 and Fig. 9. Also visible in Fig. 9 are the necks, 60 cm long and 20 cm in diameter, provided in the upper part of the cryostat. One contains the current feedthroughs and the wiring of QDS and temperature monitors. The other is for LHe supply and LHe control. Typically 18 liters of LHe are contained in the tank during magnet operation.

Magnet Operation

The magnet was completely assembled in April 1977 and first excited in May. A picture of the whole system in operating condition is shown in Fig. 10. Since no helium liquifier was available, we used a 500 liter dewar, and therefore each operating run had to be completed with that maximum total helium available.

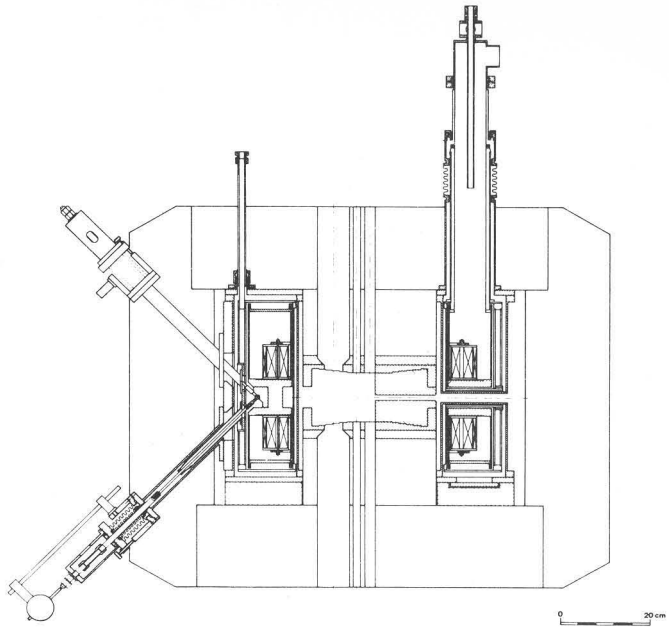

Fig. 6. Cross section of cryostat and magnet.

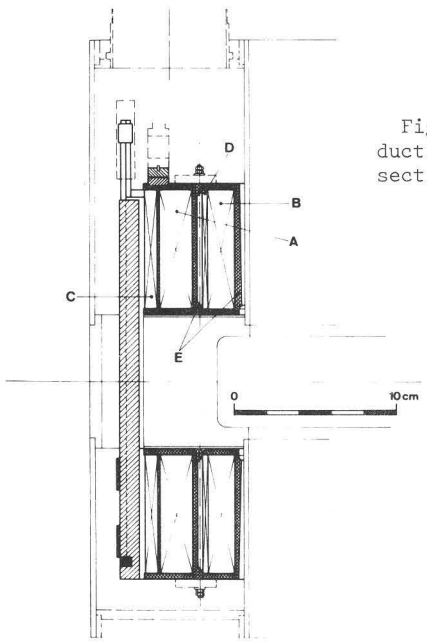

Fig. 7. Superconducting coils cross section.

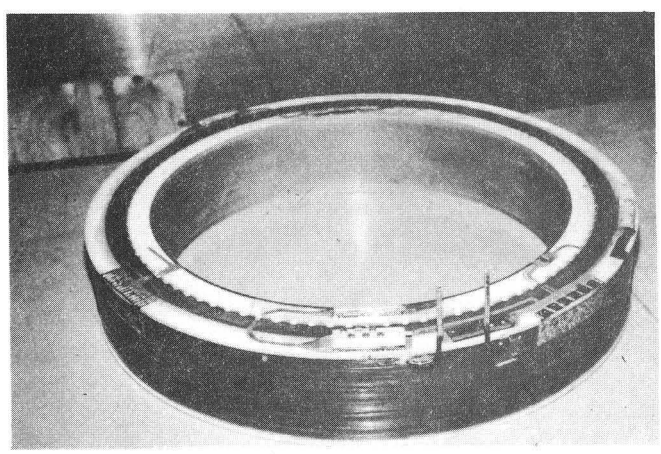

Fig. 8. Picture of the upper coil.

0018-9499/79/0400-2050$00.75 ©1979 IEEE

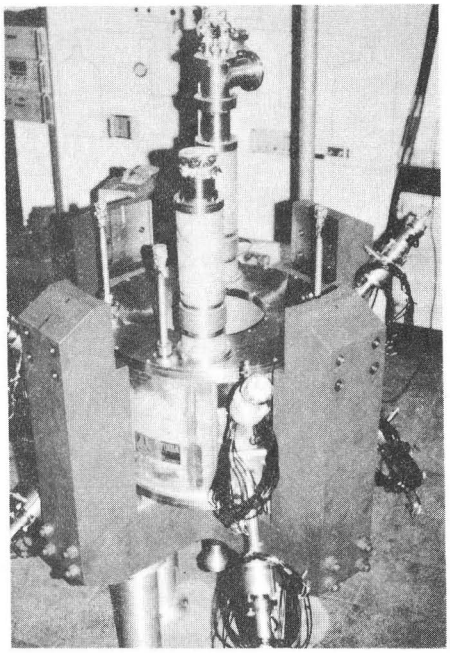

Fig. 9. Assembled cryostat.

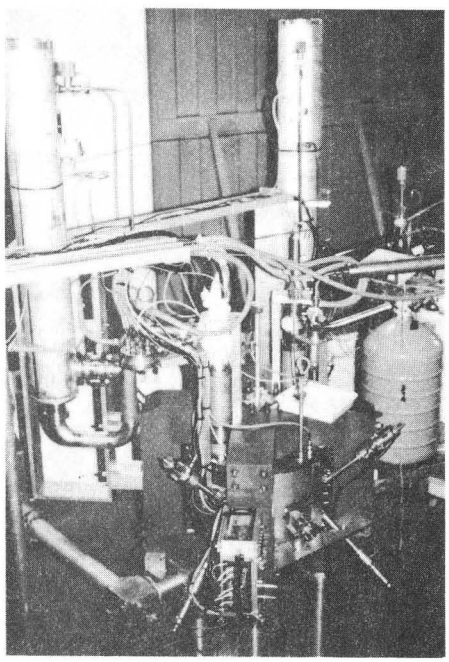

Fig. 10. Model magnet fully assembled.

Cooling of the coils and of the radiation shield to liquid nitrogen temperature is achieved in about 4 hours with the use of ≈80 liters of LN. Successive cooling to 4.2°K takes another 3 hours, and approximately 50 liters of LHe. When the filling of the cryostat is completed, the LHe level is kept constant by means of a cryoconstanter (Leybold Co.) connected to a 30ℓ dewar, visible in Fig. 10, which is periodically refilled from the 500ℓ dewar. During normal operation liquid helium consumption is usually confined to within 3 liters/hour.

As anticipated, coil training was the most demanding and time consuming part. A summary of the operating results up to now is presented in Fig. 11. As seen from the figure, a total of 8 quenches occurred before the coils were fully trained up to the maximum field.

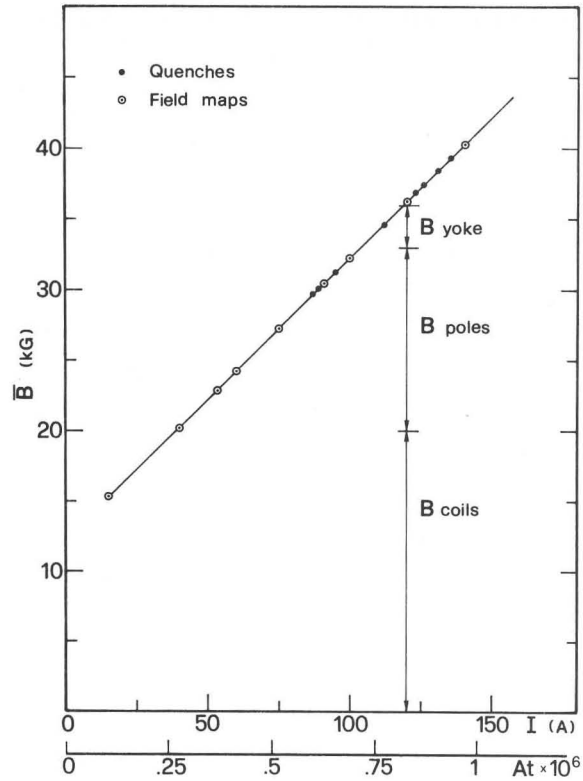

Fig. 11. Summary of coil training and magnet operation.

The training process was not, however, without problems. and we briefly comment here on the most notable events.

While the quenches up to ≈100 A were uneventful, those at a higher current, i.e. about 112 A and 126 A, where high voltages across the coils are reached (3300 V), were not without consequences. Specifically, we had a large spark tentatively traced back to a failure of voltage holding capability by a feedthrough used for the QDS. This spark generated in turn an interruption of these wires inside the cryostat. As a consequence, since the magnet can hardly be run without a failsafe QDS, it was decided to open up the cryostat and rewire the connections. This took about two months.

When operation was resumed, another quench occurring at about 120 A showed evidence of lack of insulation along the current feedthroughs near the exit from the cryostat. The energy stored in the coils discharged between the feedthrough and the cryostat wall, producing a large damage to the feedthrough itself and a local melting of the cryostat wall. This was repaired in about two weeks, with full insulation for the feedthrough assured down to the liquid helium level. At that time a decrease was observed from over 2000MΩ down to a few MΩ in the insulation resistance of the current feedthroughs, when the cold helium gas was allowed to flow through. This was traced to water condensation and ice formation on the outer parts, exposed to room environment. It was then decided to enclose the feedthroughs in sealed polyethylene caps, and to let dry nitrogen flow in. This eliminated condensation problems altogether, and resulted in a constant, 2000 MΩ insulation resistance.

When further operation was resumed, we had just three more quenches, at 121, 131, and 135.1 A. At this time, however, the quenches did not result in any inconvenience, indicating that the hardware shortcomings had been pretty much taken care of. The magnet reached successfully the max. excitation and was run stably at that level for over two hours.

0018-9499/79/0400-2051$00.75 ©1979 IEEE

In a subsequent run no more quenches occurred and magnetic field maps were taken at many different field levels, as indicated in Fig. 11, the excitation current being increased and decreased several times. Perfectly stable operation was observed for over 72 hours, indicating that the training of the coils had been effectively completed.

No problems were encountered on the cryogenics side of the operation. In particular, no leaks of any importance were observed in the cryostat. All components behaved according to specifications, with practically no trouble.

The experience gathered so far indicates therefore that the utmost care has to be placed in the design and specifications of all components which go into a superconducting magnet. The severe treatment to which the coils themselves were subjected, and which they successfully withstood, reminds that errors in this realm are not without a potentially high price tag.

Survey of Experimental Data

As mentioned above, a number of magnetic field maps have been taken, using the apparatus described in Ref. 4. For the present purposes it may just be worthwhile to recall that we employ simultaneously three Hall plates, type Siemens SBV-585-S1, with a sensitive area of 0.1 mm^2, spaced at 5 mm radial intervals. Maps are thus taken on a polar grid, with 2^o azimuthal steps, and 5 mm radial steps. The whole measuring gear is computer controlled, in order to minimize data taking time. Since a detailed description of the data is given in another paper[5] at this Conference, we shall just review here the several trends which emerge, and their implications. It is perhaps better to discuss separately the following three main aspects of magnetic field properties: i) field modulation, ii) average magnetic field, and iii) field imperfections.

Field modulation

Field modulation being essentially given by saturated pole tips, it can be taken into account as uniform surface distributions of magnetic dipoles at saturation strength. This assumption gives in fact excellent results, as shown in Fig. 12 for the coefficients of 3rd, 6th, and 9th harmonics of the magnetic field, as a function of radius, at an excitation corresponding to an average field level of 30 kG. The extensive set of data has enabled us to check the behaviour of the field modulation over a really wide range of magnetic fields. The results are shown in Fig. 13 for the 3rd harmonic amplitude at different radii, showing that the hypothesis of complete saturation holds quite well for average magnetic fields above ≈25 kG.

Average magnetic field

It is much more difficult to calculate exactly the average magnetic field, since it depends a lot on the iron magnetization of the poles and the yoke. We have not attempted very precise calculations of the yoke contribution, since our fourfold yoke symmetry prevents the use of codes like Poisson, Trim, etc. We have therefore used mainly the method of image currents, as described in Ref. 5. The results are nevertheless fairly good, as shown for example in Fig. 14, at an average field level of 35 kG. A discrepancy of about 2% on the absolute value is observed, the behaviour of B(R) vs. R being however quite consistent with the calculated one. This discrepancy is not, anyway, a very important one as far as cyclotron design is concerned, since in most cases it will involve a mere shift of the main coil excitation. Besides, calculations much more accurate than the ones presented here are possible for a real closed yoke geometry.

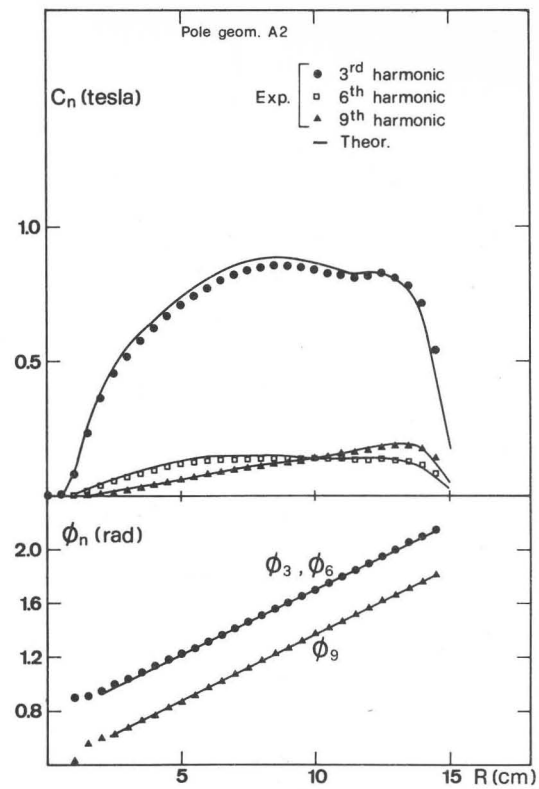

Fig. 12. Theoretical and experimental values of field harmonic amplitudes and phases.

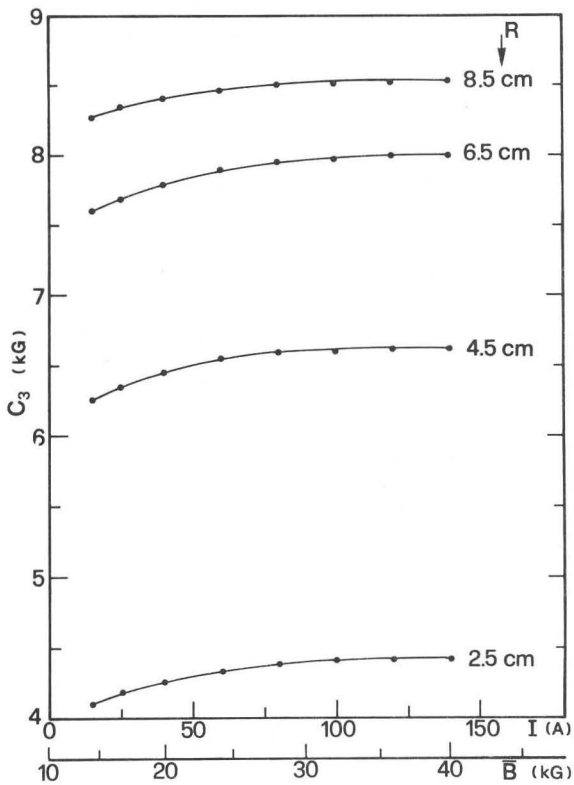

Fig. 13. Amplitude of the field third harmonics, at different radii, as a function of coil excitation.

Field imperfections

Field imperfections, mostly 1st harmonics, can be a hassle in any cyclotron, and they are particularly likely to arise in a superconducting cyclotron from

0018-9499/79/0400-2052$00.75 ©1979 IEEE

coil misalignments, since the field contribution from the coils, as shown in Fig. 14, is rather large. In our model, maps taken over 360° have indeed shown a large 1st harmonic component, as presented in Figs. 15 and 16, for excitation levels of $\simeq .55 \times 10^6$ and $.82 \times 10^6$ At respectively. Comparison of the two sets of data indicates that this 1st harmonic is due to coil mispositioning with respect to the pole, and calculations suggest the corresponding radial displacement to be of the order of 1 mm. In fact, it can also be reckoned from Figs. 15 and 16 that the phase of the 1st harmonic thus arising is practically constant, as expected from such a mechanical error. While no attempt has been made at the time of the measurements to correct for this error, this result clearly points out the need for utmost care in coil construction and positioning. Higher order harmonics, 4th and 8th, were also found, due to our peculiar yoke geometry. They are discussed in detail in Ref. 5, and are however of much less importance in the actual cyclotron design.

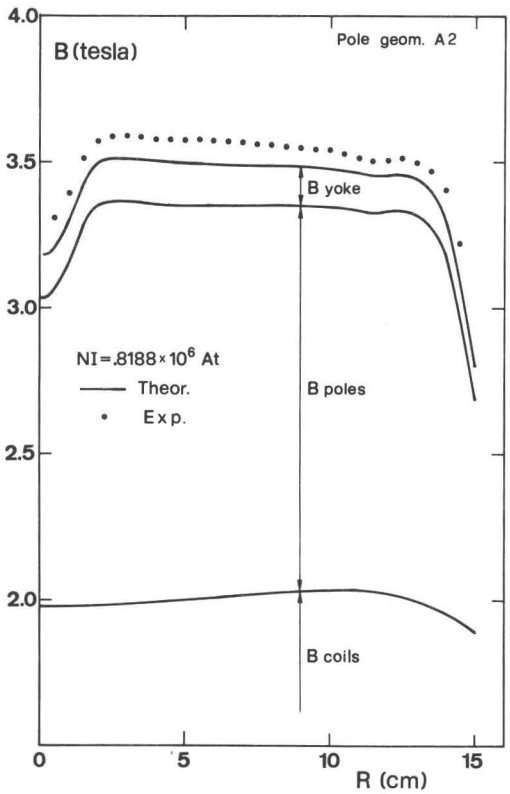

Fig. 14. Experimental (dots) and theoretical average field, as a function of radius. Contributions to the field from yoke, pole tips, and coils are also shown.

The R.F. Model

The rationale for building a 1:1 R.F. model stems out of the many uncertainties associated with the design of such an R.F. system and in particular the need to: i) verify the resonating frequency range which can realistically be obtained, ii) have fairly precise estimates of current densities at the short circuit and total R.F. power needed, and iii) verify the dee voltage distribution along the spiralling gap. It was then decided that in view of the above requirements a 1:1 scale model would best be suited. The model completely assembled is shown in Fig. 17. Since a detailed discussion of the experimental data is given in Ref. 6, we shall just summarize here the main results and consequences.

a. It was found that the cavity would resonate easily over the range of 20 to 60 MHz, but that higher frequencies would require a short circuit position too close to the median plane and therefore be impractical. Consequently, recalling the curves of Fig. 1, it was decided that the actual machine will run in the 2nd, 3rd, and 4th harmonics, the frequency range being 20 to 55 MHz. This provides a large overlap between the various harmonics, still allowing the 3rd harmonics to be used over most energies.

b. Current density on the short circuit could be limited to about 30 A/cm, thus providing a comfortable margin over acceptable upper limits (50 A/cm).

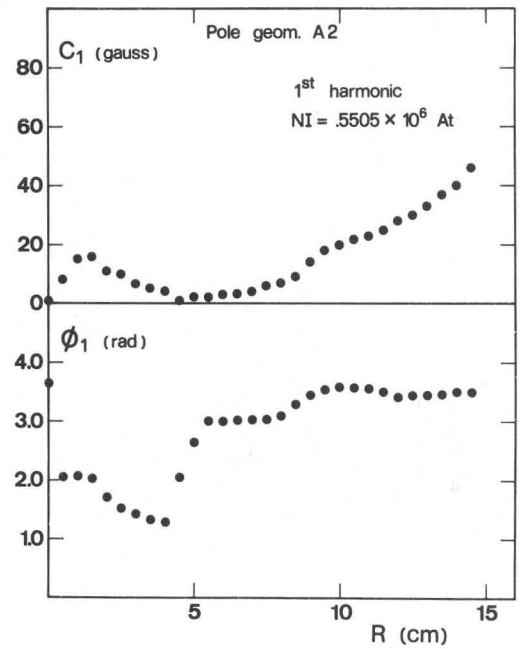

Fig. 15. Amplitude and phase of field first harmonic at .55 x 10^6 Ampereturns.

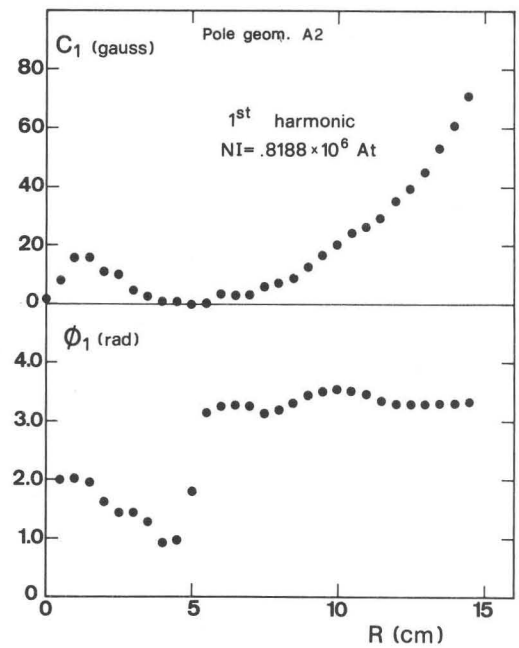

Fig. 16. Amplitude and phase of field first harmonic at .82 x 10^6 Ampereturns.

0018-9499/79/0400-2053$00.75 ©1979 IEEE

c. The total R.F. power needed for 100 kV peak dee voltage would be confined to ≃ 30 kW per cavity, so that three separate transmitters with power capability of about 50 kW each can be envisaged.

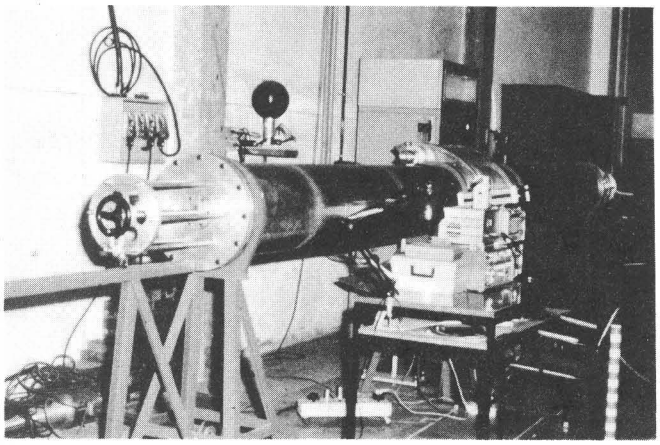

Fig. 17. The 1:1 scale model of the R.F. cavity assembled.

Project Status

As a conclusion, the model studies indicated that a superconducting cyclotron along the design lines outlined above could indeed be built. These studies and the operating experience with the models show, of course, that much care has to be placed in the design of components, probably to a much larger extent than is customary in conventional AVF cyclotrons. They also show, however, that once these technical aspects are properly handled, no real problems should arise as far as the expected machine performance is concerned.

Lack of funds in early 1978 forced this study to be discontinued and the entire project to stop. As of now, the superconducting cyclotron has been tentatively approved by the Italian National Institute for Nuclear Physics for construction within the next five year plan (1979-1984). However, no precise schedule or funding plan has been decided yet.

References

[1] E. Acerbi et al., "Studio del progetto di un ciclotrone superconductore per ioni pesanti," Report INFN, Milan, Dec. 1976, unpublished.

[2] E. Acerbi et al., "Model magnet for the proposed superconducting cyclotron at the University of Milan," IEEE Trans. Nucl. Sci. Vol. NS-24, (1977) 1109.

[3] E. Acerbi et al., "Operational experience of the 1:6 model magnet for a superconducting cyclotron," Proc. of the VI Int. Conf. on Magnet Technology, Bratislava 1977, p. 448.

[4] E. Acerbi et al., "Magnetic field measuring system for a small gap superconducting magnet," Proc. of the VI Int. Conf. on Magnet Technology, Bratislava 1977, p. 854.

[5] E. Acerbi et al., "Field measurements on the Milan superconducting model magnet," paper at this Conference

[6] C. Pagani and G. Varisco, "Model study of the R.F. cavity for the Milan superconducting cyclotron," paper at this Conference.

** DISCUSSION **

S. OHNUMA: When you repeat several cycles of cool-down and warm-up, how accurately can you reproduce the field quality?

F. RESMINI: Very precisely, since our magnet is completely saturated. Reproducibility is within the limits of our measuring accuracy.

E. HUDSON: Can you tell us something about the stray field with the open yoke structure?

F. RESMINI: We have measured it only on the median plane, up to twice the pole radius. There is of the order of 100-200 gauss—— no measurements have been made off the median plane or at larger distances.

D. LAMOTTE: Were you not interested in polishing the walls of your coil container?

F. RESMINI: No. Aluminized mylar has been used, however, all around the cryostat walls.

0018-9499/79/0400-2054$00.75